Investigating the role of smooth muscle glutamine metabolism in atherosclerotic plaque stability

Anita Salamon[1], Vlad Serbulea[2], Rebecca A. Deaton[2], Gary K. Owens[2]

[1] Department of Biochemistry and Molecular Genetics, University of Virginia

[2] Robert M. Berne Cardiovascular Research Center, University of Virginia

INTRODUCTION

- Rupture or erosion of unstable atherosclerotic plaques is the underlying cause of heart attack or stroke, which are the leading causes of death worldwide.[1]
- Stable atherosclerotic plaque has a **thick** extracellular matrix (ECM)-rich fibrous cap with a high ratio of smooth muscle cells (SMC) and myofibroblasts (MF) to macrophages (MΦ).[2]

Post-mortem association studies of left anterior descending coronary artery

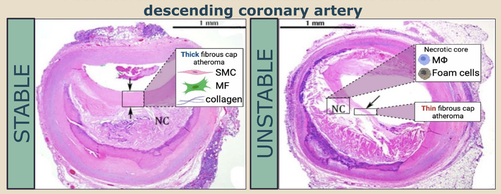

- Platelet-derived growth factor (PDGF) & Transforming growth factor-β (TGFβ)-signaling in SMC are necessary for fibrous cap formation and maintenance.[3-4]
- Analysis of 159 human carotid endarterectomies showed that glutamine (Gln) was among the most significantly changed metabolites between stable and unstable plaques.[5]
- Gln is the most abundant free amino acid in our body and its concentrations is dependent on *GS* (glutamine synthetase) and *Gls* (glutaminase) activity.[6]

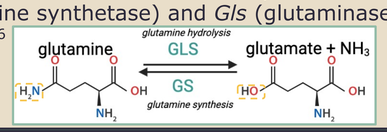

HYPOTHESIS

Glutamine availability is a critical requirement for SMC-to-MF transitions within atherosclerotic lesions, not only as a **catabolic** substrate for the energetically demanding process of ECM production but also as an **anabolic** source of proline, which comprises nearly 30% of the amino acid composition of collagen

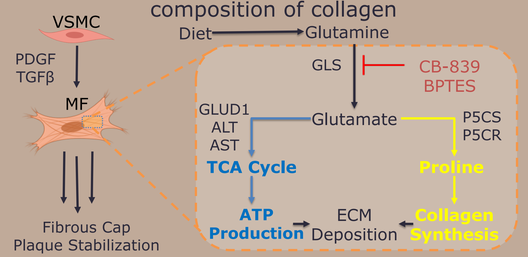

Figure 1. Visual hypothesis. Proposed mechanism of glutamine contribution to bioenergetic changes in SMC-to-MF model, in response to PDGF/ TGFβ. Glutamine is converted to glutamate via glutaminase (*Gls*). Contribution of glutamine to ECM deposition can be regulated by BPTES **(Fig. 4B),** CB-839 **(Fig. 4C)** or/and by diet **(Fig. 3).** Genes involved in glutamine-to-proline conversion **(anabolism)** include P5CS (pyrroline-5 carboxylase synthase) and P5CR (pyrroline-5 carboxylase reductase). Genes involved in ATP-production **(catabolism)** include GLUD1 (glutamate dehydrogenase), ALT (alanine aminotransferase) and AST (aspartate aminotransferase) and will be targeted in future studies to further assess glutamine contribution to SMC-to-MF transition and plaque stability in atherosclerosis.

RESULTS

1. Bioenergetic pathways were the most induced in the brachiocephalic artery (BCA) region of *Pdgfrb*$^{SMC-\Delta/\Delta}$ versus *Pdgfrb*$^{SMC-wt/wt}$ mice

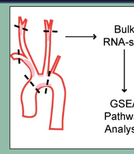

Upregulated in PDGFBR KO vs. WT	Adj. P-val
Oxidative Phosphorylation	2.2E-12
Citrate cycle (TCA cycle)	2.7E-08
Valine, leucine and isoleucine degradation	1.5E-05
Propanoate metabolism	1.9E-05
Pyruvate metabolism	2.6E-04
Fatty acid metabolism	8.1E-04
Butanoate metabolism	2.2E-03
Peroxisome metabolism	2.4E-03
PPAR signaling pathway	2.6E-03
Glyoxylate and dicarboxylate metabolism	1.0E-02

Table 1. Major transcriptional changes in energy metabolism underlie loss of SMC-PDGFRB signaling. GSEA pathway analysis showed substrate utilization and energy production pathways comprised the top 10 upregulated pathways in *Pdgfrb*$^{SMC-\Delta/\Delta}$ compared to *Pdgfrb*$^{SMC-WT/WT}$ mice fed WD for 18 weeks.

2. SMC treated with PDGF/TGFβ experience a 3-fold increase in oxidative phosphorylation compared to control, 32% of which is glutamine-derived

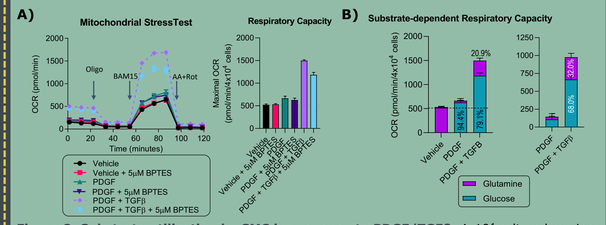

Figure 2. Substrate utilization by SMC in response to PDGF/TGFβ. 4x10^4 cultured murine aortic smooth muscle cells (mASMCs) were serum-starved for 24-72 hours prior to experiments. mASMCs were treated for 24 hours in basal medium with vehicle (4μmM HCl in PBS), 10ng/mL PDGF-BB, 10ng/mL TGFβ. **A)** Cellular respiratory capacity was assessed with a mitochondrial stress test measuring oxygen consumption rate (OCR) using DMEM media (20mM glucose; 2mM glutamine; with DMSO vehicle or 5μM glutaminase inhibitor BPTES) serially injected with ATP-synthase inhibitor oligomycin (1μM), mitochondrial uncoupler BAM15 (2μM), and mitochondrial complex III and I inhibitors antimycin A (10μM) and rotenone (1μM). **B)** The contribution of glutamine to respiratory capacity was determined by subtracting the X + BPTES condition's respiratory capacity from the X + Vehicle condition, where X is vehicle, PDGF, or TGFβ. The contribution of glucose was determined as the respiratory capacity of the X + BPTES condition. The substrate contribution to the enhanced respiratory capacity (over vehicle control) of the PDGF and TGFβ conditions is shown. Statistical significance was calculated by One-way ANOVA followed by post-hoc multiple comparison tests. (*$p < 0.05$; **$p < 0.01$)

3. Absence of glutamine results in nearly complete reduction of ECM-related gene expression

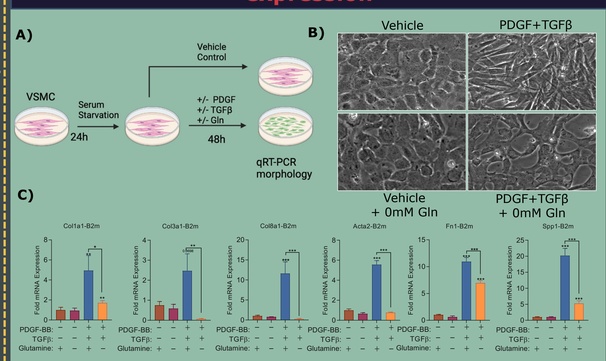

Figure 4. Transcriptional changes of SMC in response to PDGF/TGFβ and glutamine free-media. A) Schematic showing the experimental design. Briefly, mSMC were plated, serum starved, and treated with recombinant PDGF-BB/TGFβ in the absence of glutamine – 0mM vs. 2mM Gln for 48 hours followed by morphological assessment and transcriptome studies. **B)** Representative phase contrast images and **C)** mRNA expression of ECM-associated genes (standard myofibroblast panel). Graphs were analyzed using one-way ANOVA with Tukey's correction for post-hoc analysis with n≥ 3, error bars represent mean ±SEM. ***p<0.001, **p<0.01, *p<0.05

4. The glutaminase inhibitors BPTES and CB-839 decreased expression of ECM-associated genes in the SMC-to-MF system

Figure 4. Transcriptional changes of SMC in response to PDGF/TGFβ and inhibitors of glutamine metabolism. A) Schematic showing the experimental design. Briefly, mSMC were plated, serum starved, and treated with recombinant PDGF-BB/TGFβ with or without *Gls*-inhibitors: 20μM BPTES, and 1μM CB-839 for 48 hours, followed by transcriptome studies. **B)** mRNA expression of ECM-associated genes after treatment with BPTES, and **C)** CB-839 (. Graphs were analyzed using one-way ANOVA with Tukey's correction for post-hoc analysis with n≥ 3, error bars represent mean ±SEM. ***p<0.001, **p<0.01, *p<0.05

5. 50ng/ml PDGF-BB + 50ng/ml TGFb1 + 0mM Glutamine showed the strongest variation in a dataset

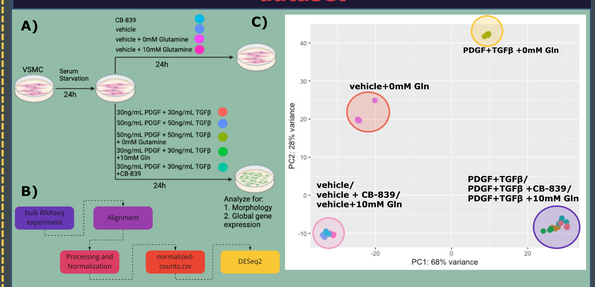

Figure 5. Principal component analysis (PCA) of SMC in response to PDGF/TGFβ and glutamine manipulations. A) Experimental design for bulk RNA-seq. mSMC were plated, serum starved, and treated with recombinant PDGF-BB/TGFβ with or without *Gls*-inhibitor CB-839, in the absence of glutamine – 0mM vs. 2mM Gln vs. 10mM Gln for 24 hours, followed by transcriptome studies. **B)** Workflow of bulk RNA-seq analysis. **C)** PCA showed the strongest separation between PDGF+TGFβ +0mM Gln(yellow circle) and PDGF+TGFβ, PDGF+TGFβ+CB-839, PDGF+TGFβ+10mM Gln (purple).

6. KEGG pathway analysis revealed that top two DOWN-regulated pathways were implicated in regulation of extracellular matrix

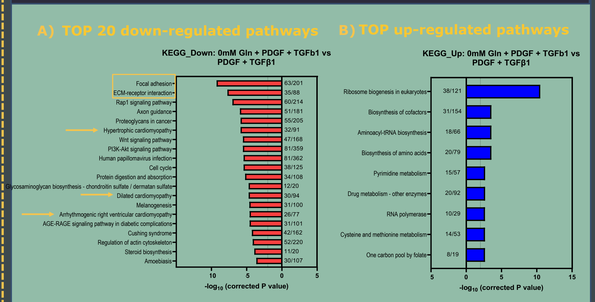

Figure 6. Pathway analysis on all significantly upregulated and downregulated genes in 0mM glutamine + 50ng/ml PDGF-BB + 50ng/ml TGFb1 vs. 50ng/ml PDGF-BB + 50ng/ml TGFb1 samples revealed novel pathways.
Bulk RNA-seq analysis was performed. Briefly, paired-end reads of 100 nucleotides in length were mapped to the mm9 reference genome using STAR v2.4. A table of gene counts/quantification was generated using FeatureCounts in the Subread package. DESeq2 Bioconductor R package was used to identify differentially expressed genes at a 1% (Padj ≤ 0.01) false discovery rate. The Benjamini–Hochberg method was used to adjust P values. Gene IDs were mapped using GENCODE/Ensembl. Significantly regulated genes were identified using the Benjamini–Hochberg procedure to adjust P values to less than or equal to 1% false discovery rate. KEGG pathway analysis was performed on all significantly **A)** downregulated and **B)** upregulated genes in the 0mM Glutamine + 50ng/ml PDGF-BB + 50ng/ml TGFb1 + 0mM versus 50ng/ml PDGF-BB + 50ng/ml TGFb1 + 0mM samples, as well as all downregulated genes based on Padj value (corrected P value).
KEGG, Kyoto Encyclopedia of Genes and Genomes.

SUMMARY

- Using oxygen consumption rate (OCR) as a measure for mitochondrial respiration, we found that 32% of the PDGF/TGFβ-induced oxidative phosphorylation in SMC is glutamine-dependent - **Fig. 2**
- Absence of glutamine led to a complete reduction of *Col8a1* and *Col3a1* (~95%) and a significant reduction of *Col1a1* and *Fn1* - 65% and 36%, respectively - **Fig. 3**
- Perturbation of glutamine metabolism with CB-839 and BPTES markedly reduced PDGF-TGFβ -induced SMC-to-MF transition – **Fig. 4**
- Glutamine starvation plus 50ng/ml PDGF-BB + 50ng/ml TGFb1 showed the strongest variation in a dataset – **Fig. 5**
- KEGG pathway analysis revealed that top two DOWN-regulated pathways were implicated in regulation of extracellular matrix– which strongly indicate that glutamine availability is critical requirement for SMC's ability to contribute to the stable ECM rich fibrous cap – **Fig. 6**
- The UP-regulated DEGs were enriched in biosynthesis pathways which emphasize the importance of glutamine that supplies carbon and nitrogen to fuel biosynthesis of nucleotides, glutathione (GSH), and other nonessential amino acids – **Fig. 6**

CONCLUSIONS

1. Glutamine is essential in the phenotypic modulation of SMC to an ECM-producing myofibroblast-state (SMC-to-MF), which forms and maintains stable fibrous caps
2. Manipulation of SMC-derived ECM-production by energetic reprogramming is of great clinical interest. We propose to alter SMC bioenergetics in vivo through pharmacologic approaches (**Fig. 4**) and through manipulation of substrate availability (**Fig. 3**)
3. SMC transitioning to MF state have increased glutamine catabolism
4. Major transcriptional changes in extracellular matrix production underlie loss of glutamine in SMC-to-MF as shown by bulk RNA-seq.
5. We propose that SMC glutamine metabolism is necessary for atherosclerotic plaque stability with the ultimate goal of identifying new therapies and dietary approaches to lower the risk of thrombotic events

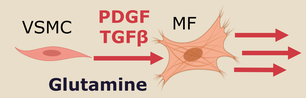

FUTURE DIRECTIONS

Question: Is glutamine availability a critical requirement for the pathogenesis in late state atherosclerotic lesion *in vivo*?

Approach : Dietary depletion of glutamine after lesion development

a. Initially feed Myh11-Cre^{ERT2}-RAD/tdTomato$^{+/+}$/*Apoe*$^{-/-}$ mice Western Diet (WD) for 18 weeks to form advanced atherosclerotic lesions
b. Then, mice will be fed custom WD without glutamine (compared to normal glutamine level for 8 weeks)
c. Expectations: decreased indices of lesion stability, including decreased fibrous cap thickness and reduced collagen content

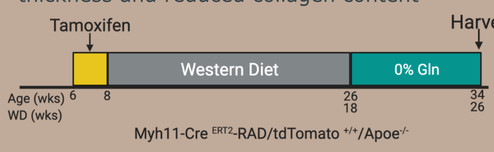

ACKNOWLEDGMENT

Bioinformativ Analysis:
Gabriel F Alencar, PhD
Laboratory Specialist:
Rupande Tripathi, MS

FUNDING:
AHA Predoctoral Fellowship
2021 – present

CONTACT

twitter.com/Anita_Salamon_
linkedin.com/in/anita-salamon
as3gd@virginia.edu

REFERENCES

1. Benjamin, E. J. *et al.* Heart Disease and Stroke Statistics-2019 Update: A Report From the American Heart Association. *Circulation.* 2019.
2. Tavora, F., Cresswell, N., Li, L., Fowler, D. & Burke, A. Frequency of Acute Plaque Ruptures and Thin Cap Atheromas at Sites of Maximal Stenosis. Arq Bras Cardiol. 2010.
3. Newman, A. A. C. *et al.* Multiple cell types contribute to the atherosclerotic lesion fibrous cap by PDGFRβ and bioenergetic mechanisms. *Nat Metab.* 2021.
4. Chen, P.-Y., Qin, L., Li, G., Tellides, G. & Simons, M. Smooth muscle FGF/TGFb cross talk regulates atherosclerosis progression. *EMBO Mol Med.* 2016.
5. Tomas, L. *et al.* Altered metabolism distinguishes high-risk from stable carotid atherosclerotic plaques. *Eur. Heart J.* 2018.
6. Albaugh, V. L., Mukherjee, K. & Barbul, A. Proline Precursors and Collagen Synthesis: Biochemical Challenges of Nutrient Supplementation and Wound Healing. *J. Nutr.* 2017.